Biosensors and Bioelectronics 119 (2018) 110–118

Contents lists available at ScienceDirect

Biosensors and Bioelectronics

journal homepage: www.elsevier.com/locate/bios

Determination of microcystin-LR, employing aptasensors

Hasan Badie Bostan[a], Seyed Mohammad Taghdisi[b], Jenna L. Bowen[c], Nikolaos Demertzis[c], Ramin Rezaee[d], Yunes Panahi[a], Aristidis M. Tsatsakis[e], Gholamreza Karimi[f,g,*]

[a] Pharmacotherapy Department, School of Pharmacy, Baqiyatallah University of Medical Sciences, Tehran, Iran
[b] Targeted Drug Delivery Research Center, Pharmaceutical Technology Institute, Mashhad University of Medical Sciences, Mashhad, Iran
[c] Cardiff School of Pharmacy and Pharmaceutical Sciences, Cardiff University, United Kingdom
[d] Clinical Research Unit, Faculty of Medicine, Mashhad University of Medical Sciences, Mashhad, Iran
[e] Department of Forensic Sciences and Toxicology, Faculty of Medicine, University of Crete, Heraklion 71003, Greece
[f] Pharmaceutical Research Center, Institute of Pharmaceutical Technology, Mashhad University of Medical Sciences, Mashhad, Iran
[g] Department of Pharmacodynamics and Toxicology, Faculty of Pharmacy, Mashhad University of Medical Sciences, Mashhad, Iran

ARTICLE INFO

Keywords:
Microcystin-LR
Aptasensor
Optical
Electrochemical

ABSTRACT

Cyanobacteria produce toxins such as microcystin-LR (MC-LR), which are associated with potential hepatotoxicity in humans. The detection of cyanobacteria and their toxins in drinking water and sea food is therefore crucial. To date, methods such as high performance liquid chromatography (HPLC), protein phosphatase inhibition assay (PPIA), and Raman spectroscopy have been employed to monitor MC-LR levels. Although these techniques are precise and sensitive, they require expensive instrumentation, well-trained personnel and involve time-consuming processes meaning that their application is generally limited to well-resourced, centralised laboratory facilities. Among the emerging MC-LR detection methods, aptasensors have received great attention because of their remarkable sensitivity, selectivity, and simplicity. Aptamers, also known as "chemical" or "artificial antibodies", serve as the recognition moieties in aptasensors. This review explores the current state-of-the-art of MC-LR aptasensor platforms, evaluating the advantages and, limitations of typical transduction technologies to identify the most efficient detection system for the potentially harmful cyanobacteria associated toxin.

1. Introduction

Cyanobacteria (blue-green algae), as gram-negative prokaryotes, are able to grow under extreme conditions including high levels of salt and UV radiation, low nutrition concentration and limited light (Kaushik and Balasubramanian, 2013). Changes in climate and accelerated eutrophication of water reservoirs may lead to cyanobacteria bloom (Abnous et al., 2017a; Žegura et al., 2011).

Microcystins (MCs) are cyclic hepta-peptide metabolites produced by species of the genera *Anabaena*, *Microcystins*, *Aphanizomenon*, *Nostoc* and *Planktothrix*, during water blooms (Liu and Sun, 2015). To date, more than 90 congeners of MCs have been identified. The different variants are mainly formed due to the presence of different α-amino acids found only at positions 2 and 4 of the molecule (Liu and Sun, 2015). Combinations between leucine (L), arginine (R) and tyrosine (Y) are able to form the common variants MC-LR, MC-RR, and MC-YR (Liu and Sun, 2015). MC-LR is the most frequently addressed member of this family, due to its abundance and potential toxicity (Lone et al., 2016).

The environmental risk of MCs in the aquatic ecosystems is significant, with the occurrence of cyanobacterial blooms in drinking water resulting in numerous public health alerts (Pham and Utsumi, 2018). The impact of MCs on animals and plants has been extensively reported via numerous studies and reviews (Pham and Utsumi, 2018). MC-LR is extremely toxic, due to its inhibitory effects on intracellular serine/threonine phosphatases 1 and 2 A (PP1 and PP2A) (Ma et al., 2016, 2017).

The mechanism of the MC uptake in plant cells remains unclear (Corbel et al., 2014). However, it is suggested that MCs are able to penetrate cell membranes via diffusion or root absorption (Peuthert et al., 2007), resulting in several disorders of plant physiology and metabolism (Smith et al., 1994). Focusing on mammalian cells, MC-LRs are absorbed through the active uptake by multispecific organic-anion transporting polypeptides (OATP), present in hepatocytes and cells lining the small intestine (McLellan and Manderville, 2017).

Humans may be exposed to MC-LR mainly through consumption of sea foods (Rezaitabar et al., 2017), agricultural plants (Miller and

* Corresponding author at: Pharmaceutical Research Center, Institute of Pharmaceutical Technology, Mashhad University of Medical Sciences, Mashhad, Iran.
E-mail address: Karimig@mums.ac.ir (G. Karimi).

https://doi.org/10.1016/j.bios.2018.08.003
Received 12 June 2018; Received in revised form 1 August 2018; Accepted 2 August 2018
Available online 08 August 2018
0956-5663/

Russell, 2017) and drinking water (Gaget et al., 2017), leading to illnesses and deaths. For example, 70 deaths were confirmed due to direct exposure to MCs during the “Caruaru Incident” in Brazil in 1996 (Liu and Sun, 2015). Additionally, the International Agency for Research on Cancer (IARC) categorized MC-LR as possible human carcinogen (Group 2B) (Li et al., 2017b; Lundqvist et al., 2017). Apart from the liver, the testis is another target organ for MC-LR; its presence not only disrupts motility and morphology of sperm but also alters male hormone levels (Lone et al., 2015; Zhang et al., 2017a). Moreover, immunotoxicity (Chen et al., 2017), genotoxicity (Zegura, 2016), and developmental toxicity (Qi et al., 2016) associated with this cyanotoxin has been investigated.

The World Health Organization (WHO) has set a cut-off concentration of 1 $\mu g\ L^{-1}$ as an acceptable level for MC-LR in drinking water (He et al., 2017; Zhang et al., 2017b). To date MC-LR is the only cyanotoxin to receive such guidance, highlighting its toxicological profile (Turner et al., 2018). Thus, the development of sensitive analytical methods for detection of MC-LR is greatly needed. Low concentrations and different isoforms of MCs in environmental samples present significant analytical challenges (Zanato et al., 2017; Zhang et al., 2017b). Various analytical approaches such as high performance liquid chromatography (HPLC), protein phosphatase inhibition assays, and enzyme-link immunosorbent assay (ELISA), have been employed for MC-LR determination (Hu et al., 2017; Qileng et al., 2018). Although these techniques are commonly accepted, the assays are time-consuming and require complicated and costly instrumentation, which somewhat limits their application (Liu et al., 2017a; Wei et al., 2017). It also means that testing has to be performed within a central laboratory, rather than at the source of suspected MC-LR contamination. On the other hand, the development of novel biosensor platforms has enabled the reproducible, and accurate detection of MC-LR in a portable format (Qileng et al., 2018).

Aptamers are single-stranded nucleic acid sequences that recognize their targets with remarkable affinity and selectivity (Nimjee et al., 2017). These so-called “chemical antibodies” are produced through an in vitro process named Systematic Evolution of Ligands by EXponential enrichment (SELEX) (Nimjee et al., 2017). From a historical point of view, the first aptamer for MC-LR detection was developed by Nakamura and co- workers in 2001 (Nakamura et al., 2001). This aptamer could perform label-free detection of MC based on surface plasmon resonance and had a detection range of 50 $\mu g\ mL^{-1}$ to 1 $mg\ mL^{-1}$. The poor detection limit of the proposed aptasensor was attributed to its low affinity. In 2004, Gu and co-workers used different aptamers for detection of MC-LR. Among the different RNA aptamers used, MC25 clone RNA showed relatively high affinity and it was able to react with MC-LR at concentrations as low as 0.5 $\mu mol\ L^{-1}$ (Gu and Famulok, 2004).

In 2012, Ng and co-workers proposed various sequences for MC-LR, MC-LR, and MC-YR detection with different affinities. Among them, a 60-mer sequence, named AN6, exhibited the best selectivity ($K_d = 50 \pm 12$ nM) towards MC-LR. Because of its favorable properties, this aptamer was employed in different MC-LR aptasensors (Ng et al., 2012).

In comparison to their protein counterparts, aptamers offer several advantageous characteristics including lack of immunogenicity, ease of synthesis and modification, and low molecular weight (Lyu et al., 2016).

Aptasensors are biosensors in which an aptamer is employed as the recognition moiety (Hosseini et al., 2015). To date, numerous aptasensors have been designed for detection of toxins (Li et al., 2017a), viruses (Ghanbari et al., 2017), bacteria (Brosel-Oliu et al., 2017) proteins (Bini et al., 2008), metals (Taghdisi et al., 2015) and drugs (Abnous et al., 2017a) in different matrices. In recent years, a number of aptasensors for the detection of MC-LR have been developed (Abnous et al., 2017b; Taghdisi et al., 2017).

Nanomaterials (NMs) are regarded as a promising agents for construction of aptasensors, due to their physico-chemical properties such as disposability, small size, and high surface area. For instance, carbon NMs are involved in sensing systems, because of their pronounce biocompatibility and electrical conductivity (Rowland et al., 2016). Additionally, magnetic NMs are able to extract and concentrate a target compound from a complex matrix.

This review aims to discuss the state-of-the-art of MC-LR aptasensors. Key performance indicators such as sensitivity, accuracy, robustness and cost-effectiveness of such aptasensors are evaluated.

2. Aptasensor-based optical detection of MC-LR

Optical aptasensors involve aptamers as the recognition element and an optical-based technique as the transducer. Unique features such high sensitivity, fast response and ease-of-use led to extensive application of optical aptasensors for monitoring toxin levels. Colorimetric (Abnous et al., 2017b), fluorescent (Taghdisi et al., 2017), and surface-enhanced Raman scattering (SERS) (Hassanain et al., 2017) are examples of optical systems that have been used to develop aptasensors for MC-LR detection.

2.1. Colorimetric aptasensors for MC-LR detection

Colorimetric-based biosensors are arguably the simplest of the sensing systems, providing good performance with simple to use and cost-effective technologies. The possibility of detection with the naked eye is also appealing, with such sensors representing a ‘low-tech’ solution that is deployable across resource poor-settings (Ansari et al., 2017).

The aggregation potential of gold nanoparticles (AuNPs) has been utilized in the sensing of various analytes (Bostan et al., 2017); the colour of the solution varies as a consequence of particle aggregation, which in turn is influenced by the presence of analytes (Ansari et al., 2017).

Exploiting this phenomenon, Li and co-workers developed a highly sensitive colorimetric aptasensor for detection of MC-LR in water. As shown in Fig. 1, modifying the surface of AuNPs with aptamers prevents the electrostatically induced aggregation of AuNPs in high salt concentrations from occurring. Without aptamer modification, elevated salt concentrations bring about aggregation which manifests as a change in colour of the solution. Upon addition of MC-LR (the target analyte) to the aptamer-modified AuNPs, a violet-blue colour is observed as the specific interaction between aptamer and its target (Fig. 1C). No change in colour is observed when the system is challenge with competitor analytes, thus demonstrating sensor selectivity. The recoveries ranged from 98.5% to 102.2% and standard deviation varied from 7.4% to 10.7%, demonstrating a good accuracy for this sensing system (Fig. 1D) (Li et al., 2016b).

Compared to other techniques, colorimetric-based biosensors relying on assembly/disassembly of aggregates generally demonstrate limited dynamic responses with relatively low sensitivities (e.g. limit of detection in sub-nanomolar or nanomolar range) (Wang et al., 2015). However studies have shown that disassembly of preformed AuNP aggregates, can enhance the sensitivity and time-to-result of the systems (Song et al., 2011; Waldeisen et al., 2011). Recently, Gue and co-workers showed that forming AuNP-dimers, as opposed to larger scale aggregates, results in an improvement of not only the sensitivity but also the dynamic range and long-term stability of such colorimetric-based biosensors. Additionally, they have shown that formation of a Y-shaped DNA duplex upon dimer formation, mimises the inter-particle distance such that a significant improvement in LOD is achievable (Guo et al., 2013). A crucial challenge in development of AuNPs sensing platforms, is the "corona shield effect" which could be overcome by utilization of polyethylene glycol (PEG) (Danesh et al., 2017).

Such an approach has been used to develop a colorimetric-based aptasensor for the detection of MC-LR with an LOD value of 0.05 nM (Wang et al., 2015). In this study, AuNPs were first functionalized with

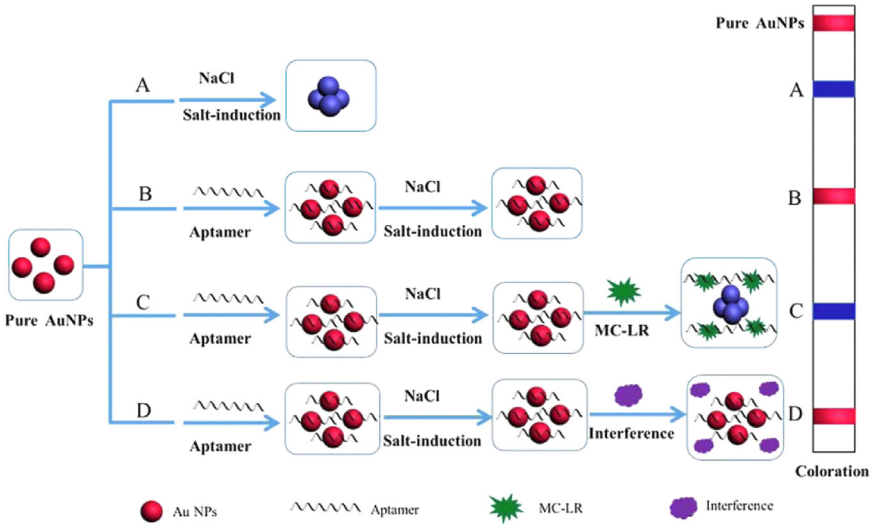

Fig. 1. Colorimetric-based aptasensor for detection of MC-LR in water, developed based on aggregation/disaggregation properties of AuNPs. Copied from the study of Li et al. (Li et al., 2016b) with permission.

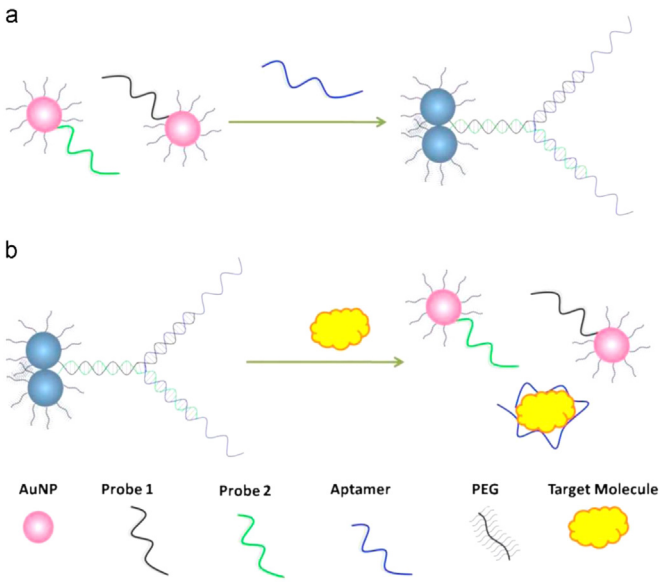

Fig. 2. Schematic diagrams showing the production and disassembly of AuNP dimers. In the absence of the target, the complex of functionalized AuNPs and aptamer produced a Y-shaped structure. Addition of MC-LR resulted in disruption of Y-duplex and changes in solution colour. Copied from the study of Wang et al. (Wang et al., 2015) with permission.

PEG and two probe oligonucleotides (probes 1 and 2, Fig. 2), to which an aptamer was added (Fig. 2a), Addition of the aptamer resulted in the formation of a Y-shaped duplex and dimerisation of AuNPs which was observed as a blue solution. Addition of the target molecule (MC-LR) results in disruption of the Y-duplex as the aptamer preferentially interacts with its target. Consequently, the AuNP dimers dissociate and a colour change is observed within 5 min (Fig. 2b). This aptasensor exerts its maximum performance at temperatures ranging from 15° to 35°C and at higher temperatures remarkable signal decreases are observed. This reduction of signal, which is regarded as a major drawback in such sensing systems, is caused by alterations of DNAs affinity at relatively high temperatures (Wang et al., 2015).

A colorimetric aptasensor was developed for determination of MC-LR based on a hairpin aptamer, graphene oxide (GO) hydrogel, methylene blue (MB), complementary strand (CS) and streptavidin-modified magnetic particles (SMPs). In this assay, MB, SMPs, aptamer, CS and adenosine acted as dye, immobilizer, recognition probe, and GO gelation promoters, respectively. Graphene oxide (GO) is a nanomaterial produced by oxidation of graphene. Characteristics such as high water dispersibility and thermal conductivity, make it a popular material for incorporation in biosensors. Importantly, there are intense interactions between bases of single-stranded oligonucleotides and hexagonal cells of GO. This interaction not only protects oligonucleotides from nuclease cleavage, but also quenches the fluorescence of dyes (Ling et al., 2016). The hairpin structure of the aptamer helps to maximise selectivity. In the absence of the target analyte, the gelation process of GO is increased by the presence of the CS and adenosine, and MB remains between the GO sheets. However, in the presence of MC-LR, the less robust hydrogel structure allows MB to leach out from the hydrogel, imparting a blue colour to the solution which can be measured spectroscopically. This system provides a limit of detection (LOD) of 221 pM and 412 pM in spiked tap water and serum samples, respectively (Abnous et al., 2017b). Recovery values ranged between 91 ± 8.1 and 98.2 ± 6.7%, suggesting a good reliability for the proposed aptasensor.

Although GO represents favorable properties, synthesis of this nanoparticle needs expertise. In addition, when GO is applied for detection of a given compound in serum samples, sensitivity of the sensing platform may vary due to interactions between GO and proteins. This problem can be overcome by pretreatment of GO with molecules like polyethylene glycol (PEG) and albumin (Danesh et al., 2017).

2.2. Fluorescent aptasensors for MC-LR detection

In general, two approaches are used in the development of fluorescence-based aptasensors. The first is based upon directly labeling the aptamers with fluorophores to generate so-called 'signaling aptamers', while the second involves labeling the aptamer with a molecule designed to quench fluorescence in fluorescence resonance energy transfer (FRET) approaches (Shahdordizadeh et al., 2017). FRET occurs as a result of non-radiative energy transmission between donor fluorophore and acceptor molecule (chromophore/fluorophore) (Sekar and Periasamy, 2003). FRET can be utilized to explore binding dynamics, molecular interactions as well as biomolecular conformation (Sahoo, 2011).

Various donor and acceptor fluorophores including inorganic nanostructures, fluorescent proteins, and organic dyes, have been exploited in the generation of fluorescence based aptasensors (Jamali et al., 2014). Recently, a novel aptasensor was designed using single-

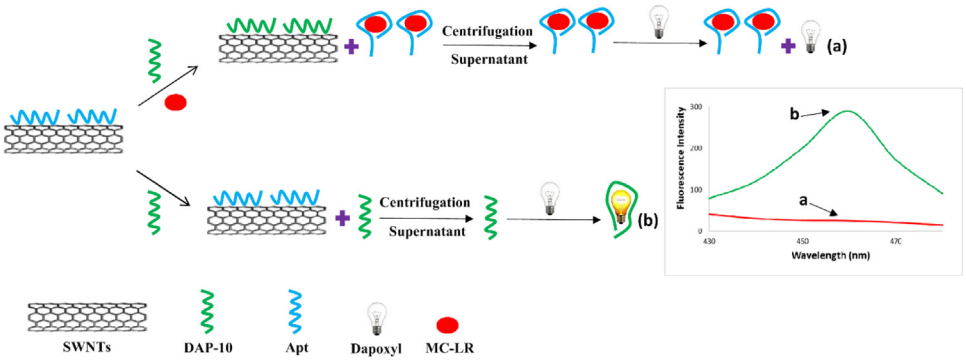

Fig. 3. Schematic presentation of MC-LR determination based on a fluorescent approach. In the presence of MC-LR, Apt binds MC-LR and leaves the surface of SWNTs. So, DAP- 10 could bind the surface of SWNTs, resulting in a weak fluorescence intensity (a). In the absence of MC-LR, the Apt remains on the surface of SWNTs and DAP-10 could not bind the surface of SWNTs, leading to a strong fluorescence intensity (b). Copied from the study of Taghdisi et al. (Taghdisi et al., 2017) with permission.

walled carbon nanotubes (SWCNTs). SWCNTs are allotropes of carbon which consist of a sheet of graphene (Bostan et al., 2016). Extraordinary features such as high surface area, excellent mechanical and thermal stability, and electrical conductivity justify widespread application of SWCNTs in biosensors (Herrero-Latorre et al., 2015; Jain et al., 2015). In the study by Taghdisi et al., SWCNTs were used as a solid support to which two aptamers, one targeting MC-LR and the other targeting a fluorescent dye (dapoxyl), could bind (Fig. 3). If the anti-MC-LR aptamer is bound to the surface of the SWCNTs (i.e. in the absence of MC-LR) the anti-dapoxyl aptamer is able to form a complex with the dye which produces as strong fluorescent signal. When MC-LR is present, the originally surface bound MC-LR aptamer dissociates from the SWCNTs allowing the anti-dapoxyl aptamer to bind the carbon nanotube, which results in a substantial attnetuation of the fluorescence intensity. Under optimal conditions, this aptasensor demonstrated highly sensitive detection of MC-LR with a LOD of 138 pM Good recoveries were achieved for serum samples (between 88.46 ± 2.6 and 103.7 ± 8.4%) reflecting high reliability and accuracy for this aptasensor (Taghdisi et al., 2017).

As a relatively new generation of nanomaterials, upconversion nanoparticles (UCNPs) have demonstrated unique optical properties including low background, remarkable luminescence and lack of autofluorescence. Consequently these materials provide a good alternative to traditional fluorescence based readouts for bioassays (Nguyen et al., 2014). When UCNPs are doped with lanthanide ions, they show interesting properties such as prominent visible luminescence emission (Wu et al., 2015).

Wu and co-workers fabricated an aptasensor that could detect MC-LR and okadaic acid (OA), using a dual FRET system (Wu et al., 2015). They employed NaYF4: Yb, Ho UCNPs and Mn^{2+}-doped NaYF4: Yb, Er UCNPs as donors. Two Black Hole Quencher® species (BHQ1 and BHQ3) were used as the acceptors. In this system, specific MC-LR and OA aptamers were attached to the NaYF4: Yb, Ho UCNPs and Mn^{2+}-doped NaYF4: Yb, Er UCNPs, respectively. Each donor-acceptor couples were produced by hybridizing the aptamers with their specific cDNA. In the absence of the targets, upconversion luminescence is quenched by acceptors. On the other hand, when analytes were added to the system, luminescence values were increased. The linear range of aptasensor was between 0.1 and 50 ng mL^{-1}. Additionally, recovery ranged from 97.68% to 120.1% in shrimp, fish and water matrices. RSD of this sensing interface at 10 ng mL^{-1} was 6.47% (n = 7), which indicated that the proposed analytical method has a good reproducibility. This technique had the potential of monitoring MC-LR and OA in foodstuff and environment, simultaneously (Wu et al., 2015).

Although FRET-based reporters are extensively used, they may have various limitations. For instance, physical vicinity between donor and acceptor and weak signal-to-noise ratio are known as important downsides of them (Nosrati et al., 2018). In addition, matrix condition such as temperature, pH, and ionic concentrations may affect fluorescence intensity. By means of time-resolved fluorescence, this limitation can be solved (Danesh et al., 2017).

Molybdenum disulfide (MoS_2) is an inorganic compound which is classified as transition metal dichalcogenide (TMDC) (Woods et al., 2016). It displays marked conductivity and fluorescence quenching, which coupled with its strong affinity toward single-stranded DNA / aptamers, make it a valuable material for inclusion in biosensors (Liu et al., 2014; Shuai et al., 2017). Exploiting the enhanced fluorescence of core/shell UCNPs and quenching property of MoS_2, a simple sensitive aptasensor for MC-LR was developed with an LOD value of 2 pg mL^{-1} (Fig. 4). In this system, the aptamer was immobilized on core/shell-UCNPs, which were subsequently adsorbed onto MoS_2 through van der Waals interactions via the nucleobases. Whilst adsorbed, energy is transferred from the core/shell-UCNPs to the MoS_2 which results in quenching of the fluorescence. In the presence of the target (MC-LR), an aptamer – target complex is formed, which results in desorption form MoS_2 leading to recovery of fluorescence. The linear range of this aptasensor was determined to be 0.01–50 ng mL^{-1}. The recovery values ranged between 94% and 112% (with minimal RSD), reflecting excellent recovery and reproducibility of this method (Lv et al., 2017).

2.3. Surface Enhanced Raman Scattering (SERS) aptasensors for MC-LR detection

SERS is an oscillatory spectroscopic method which integrates molecular fingerprints of Raman spectroscopy technique with potential single-molecule sensitivity (Cialla et al., 2012). In this system, following adsorption of the desired compound on a nanostructured coinage metal surface, Raman scattering is increased (Mosier-Boss, 2017). Such approaches are associated with a number of perceived advantages including speed, the label free, non-destructive testing of

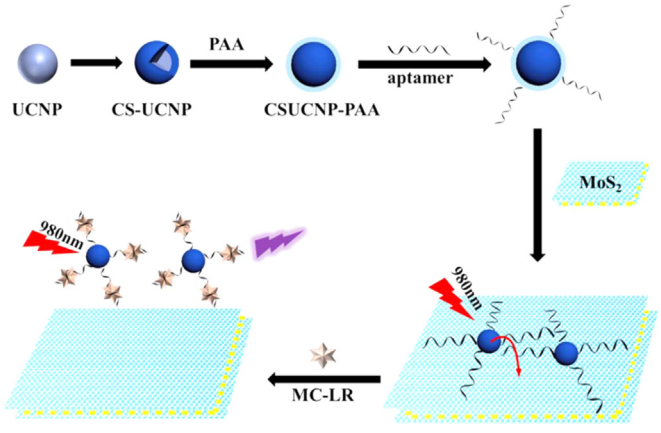

Fig. 4. Schematic illustration of fluorescence aptasensor developed for determination of MC-LR. In this sensing interface, an specific aptamer was immobilized on core/shell-UCNPs and then introduced to the MoS_2. In this structure, MoS_2 quenched fluorescence of core/shell-UCNPs. Addition of target resulted in desorption from MoS_2 surface and fluorescence recovery. Copied from the study of Lv et al. (Lv et al., 2017) with permission.

samples as well as the ability to simultaneously analyse different targets, however reproducibility remains a challenge (Fisk et al., 2016).

Highly branched tips of gold nanoflowers (AuNFs) exert high surface to volume ratio (Yi et al., 2013). AuNFs not only yield stable SERS signal, but also show remarkable electromagnetic field improvement (La Porta et al., 2015). Additionally, SERS activity is increased by silver (Ag) surfaces. Using (AuNF)-AgNP core- satellite assemblies, Zhao and co-workers produced a Raman aptasensor with amplified SERS signal and high sensitivity (LOD = 8.6 pM) (Zhao et al., 2015). For production of these SERS active assemblies, AuNF and AgNP probes were hybridized with MC-LR aptamers. Following introduction of the target, those assemblies were destroyed leading to signal reduction. The recovery rates ranged from 94.48 ± 3.42–97.70 ± 3.56%. Good recovery and low RSD insured that this sensing platform has acceptable accuracy and reproducibility (Zhao et al., 2015).

Poor selectivity is an important drawback in label-free SERS methods (Hassanain et al., 2017). To overcome this problem, several clean-up and extraction steps are needed (Hassanain et al., 2017).

2.4. Electrochemiluminescence (ECL) aptasensors for MC-LR detection

Electrogenerated chemiluminescence, particularly known as ECL, involves excited states at or near electrode surfaces (High et al., 2001). ECL offers several advantages including wide range of targets, low background signal, and cost-effectiveness (Zhou et al., 2011). Three-dimensional graphene hydrogels (3D GHs), as a new generation of ultralight and porous carbon-based materials have attracted extensive attention. 3D GHs not only represent high surface to volume ratio, but also provide special sites for ECL luminophore molecules assembly (Du et al., 2016c).

Recently, an ECL aptasensor was designed with an LOD of 0.03 pM (Du et al., 2016c). In this case, boron and nitrogen co-doped graphene hydrogels (BN-GHs) were used to amplify steric hindrance between MC-LR and its specific aptamer. Additionally, quartz crystal microbalance (QCM) was applied to investigate these events. Linear range of proposed platform was determined from 0.1 pM to 1000 pM This sensing system does not require high price labeling and complicated probe immobilization stage. After incubation of aptasensor with 5 pM, an RSD of 5.3% was obtained (n = 12), suggesting a good repeatability (Du et al., 2016c).

In general, optical aptasensor-based platforms have remarkable merits Like feasibility of quantitative analysis without need for advanced devices. Colorimetric aptasensors are able to detect targets and used with the naked eye. In spite of advancements in optical aptasensors, they still have limitations such as requirement of time- consuming processes and low portability (Nosrati et al., 2017). Table 1 exhibits the characteristics of optical-based aptasensors.

3. Electrochemical-based aptasensors for MC-LR detection

In the case of electrochemical aptasensors, the aptamer is immobilized directly onto the electrode surface and target-aptamer interactions are monitored using a number of electrochemical transduction approaches (Meirinho et al., 2016). Molecular interactions that occur at the electrode surface manifest as measurable changes in electrical output such as impedance, voltage, and current (Wang et al., 2016).

In comparison with optical methods, electrochemical transduction offers several benefits including ease of miniaturization, compatibility with novel microfabrication technologies, fast response, simplicity, etc. (Meirinho et al., 2016). To date, a number of different electrode surfaces such as glassy carbon electrodes (GCE), screen printed electrodes (SPE), and carbon paste electrodes (CPE) have been applied for designing electrochemical aptasensors (Meirinho et al., 2016).

In 2014, an electrochemical aptasensor targeting MC-LR was fabricated using graphene-modified SPE. Herein, the anti-MC-LR aptamer

Table 1
Optical-based aptasensors.

Detection method	Strategy	LOD (ng mL^{-1})	Linear range	Aptamer/K_d	Ref.
Colorimetry	Based on disassembly of orient-aggregated gold nanoparticle dimers	0.0497	0.0995–248.797	5′-GGC GCC AAA CAG GAC CAC CAT GAC AAT TAC CCA TAC CAC CTC ATT ATG CCC CAT CTC CGC-3′ [sequence A (K_d = 50 ± 12 nM)]	(Wang et al., 2015)
Colorimetry	AuNPs aggregation in the presence of salt	0.3682	0.4975–7463.917	sequence A	(Li et al., 2016b)
Colorimetry	Employing aptamer, graphene oxide, and methylene blue acting as an optical probe	0.2179	0.6468–995.189	5′-GGG TGG GTG GGG GGC GCC AAA CAG GAC CAC CAT GAC AAT TAC CCA TAC CAC CTC ATT ATG CCC CAT CTC CGC CCC CAC CCA CCC − 3′ (K_d not mentioned)	(Abnous et al., 2017b)
Fluorescence	Using two donor (upconversion nanoparticles) and acceptor (BHQ1 and BHQ3) couples	0.025	0.1 − 50	sequence A	(Wu et al., 2015)
Fluorescence	Single-walled carbon nanotubes (SWNTs) as immobilizers, dapoxyl as a fluorescent dye	0.1373	0.398–1194.22	sequence A	(Taghdisi et al., 2017)
Fluorescence	Using the enhanced fluorescence of core/shell (CS) UCNPs and quenching property of MoS_2	0.002	0.01–50	sequence A	(Lv et al., 2017)
Surface-enhanced Raman scattering (SERS)	Using gold nanoflower-Ag NP core- satellite assemblies as signal amplifier	0.0085 ± 0.0003	0.0099–9.9518	Not disclosed	(Zhao et al., 2015)
Electrochemi-luminescence (ECL)	Steric hindrance initiated signal amplification effect	0.00003	0.0001–0.9951	sequence A	(Du et al., 2016c)

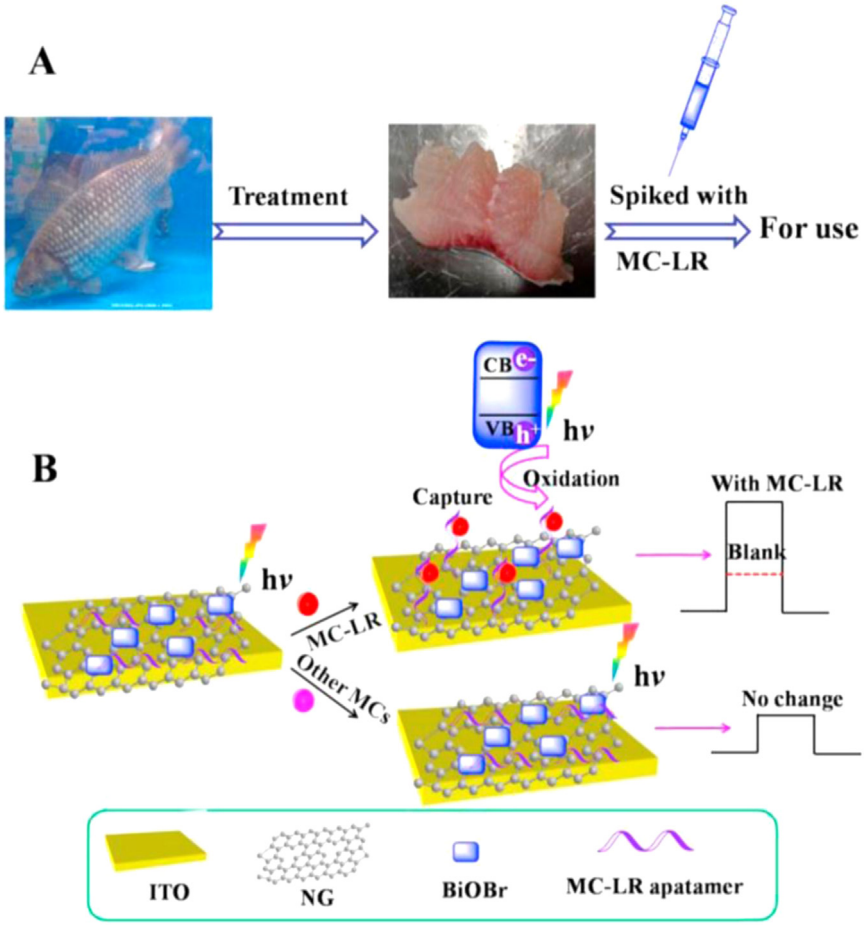

Fig. 5. Schematic illustration of PEC aptasensing system developed using BiOBrNFs-NG/ITO electrode. In this aptasensor, visible light-responsive materials were introduced by immobilization of BiOBrNFs-NG nanocomposites on electrode. Copied from the study of Du et al. (2016a) with permission.

was simply adsorbed on the electrode surface by exploiting the π-π stacking interactions between nucleobases of DNA aptamer and cells of graphene. It was observed that following the non-covalent modification of the electrode with the aptamer, the square wave voltammetric (SWV) reduction signal of the $[Fe(CN)_6]^{4-/3-}$ redox couple dropped. Introduction of target to the aptasensor led to dose-dependent increases in peak current. The system demonstrated high sensitivity and selectivity with a LOD of 1.9 pM (in buffer). Recovery rate of this system was 98.1% and 91.7% in spiked fish extract and tap water, respectively. (Eissa et al., 2014).

Desirable advantages like ease of operation and good sensitivity make electrochemical impedance spectroscopy (EIS) a popular measurement approach in the generation of aptasensors (Hayat et al., 2013; Lin et al., 2013; Randviir and Banks, 2013; Rivas et al., 2015). Combining the advantages of aptamer-based recognition and EIS resulted in the development of a label- free aptasensor by Lin and co-workers, for detecting of cyanobacterial toxin MC-LR in water samples (Lin et al., 2013). In the proposed system, MC-LR aptamers with immobilised onto gold electrodes, to form a monolayer with relatively high electrochemical impedance. Upon binding with the target analyte, the aptamers underwent a conformational change, which allowed easier transfer of an external redox mediator, $[Fe(CN)_6]^{3-/4-}$, to the electrode surface. This manifests itself as a reduction of the apparent impedance of the system. Over the range of 1.0–5.0 × 10^{-11} mol L^{-1}, a linear relationship was observed between MC-LR concentration and electrochemical impedance changes. The LOD of this sensing model was determined to be 1.8 × 10^{-11} mol L^{-1}, whilst sample recovery was in the range of 91.2–113.7%. Low relative standard deviation (RSD) value of the resulting impedances (3.52%) indicated that the fabricated sensing system has good reproducibility (Lin et al., 2013).

In another study, cobalt (II) salicylaldiimine metallodendrimer (SDD–Co(II)) was doped with AgNPs to design a electrochemical aptasensor for MC-LR detection at nanomolar levels (Bilibana et al., 2016). In the proposed system, a thin film of SDD–Co (II) was deposited onto a GCE surface and then AgNPs were electro-synthesized on the surface of film. A 5′ thiolated DNA aptamer was subsequently encouraged to self-assemble on AgNPs. The sensing platform demonstrated linearity between 0.1 and 1.1 μg L^{-1} with a LOD of 0.04 μg L^{-1}. Employing standard spiking methods, the average recoveries were calculated as between 94% and 115% in water samples (Bilibana et al., 2016).

In 2012, Ng and co-workers fabricated electrochemical aptasensors using three different aptamers to monitor microcystin congers. Here, 5'-disulfide-terminated aptamers were immobilized on the gold electrode and then exposed to redox cations ($[Ru(NH_3)_6]^{+3}$). This led to high reduction peak current of $[Ru(NH_3)_6]^{+3}$. When analytes were added to the system, significant decreases in reduction peak current were observed. The aptasensor, which employed an AN6 sequence (GGCGCC AAACAGGACCACCATGACAATTACCCATACCACCTCATTATGCCCCAT CTCCGC), was able to detect MC-LR with an LOD of 11.8 p.M. Linear responses were observed from 10 p.M. to 10 nM (Ng et al., 2012).

In recent years, the photoelectrochemical (PEC) technique has gain marked attention. PEC benefits from the advantage of electrochemical method and uses an optical approach (the advantages of both electrochemical and optical techniques have been noted above) (Du et al., 2016b). High sensitivity, simplicity of miniaturization, low-cost and simple equipment are examples of PEC merits (Okoth et al., 2016).

Photocatalysts play an essential role in the PEC technique, as they

Table 2
Electrochemical-based aptasensors.

Detection method	Strategy	LOD (ng mL^{-1})	Linear range	Aptamer/K_d	Ref.
Square wave voltammetry (SWV)	5-disulfide terminated aptamers immobilized on the gold electrode	0.0117	0.0099–9.9518	sequence A	(Ng et al., 2012)
Electrochemical impedance spectroscopy (EIS),SWV	Unlabeled DNA aptamer anchored on a graphene electrode	0.0018	0.0001–0.9951	sequence A	(Eissa et al., 2014)
EIS, Cyclic voltammetry (CV)	Cobalt (II) salicylaldiimine metallodendrimer (SDD–Co(II)) doped with AgNPs	0.04	0.1–1.1	sequence A	(Bilibana et al., 2016)
EIS	BiOBr nanoflakes/N-doped graphene (BiOBrNFs-NG) provided as a visible light-responsive material	0.00003	0.0001–99.518	sequence A	(Du et al., 2016a)
EIS	Aptamers immobilized on graphene functionalized titanium dioxide nanotubes (TiO_2 NTs)	0.0000005	0.000001–0.00047	sequence A	(Liu et al., 2016)
CV, EIS	Immobilization of MC-LR aptamers on the gold electrode	0.0179	0.0099–0.0497	5′-TTT TTG GGT CCC GGG GTA GGG ATG GGA GGT ATG GAG GGG TCC TTG TTT CCC TCT TG− 3′ (K_d= 0.5 micromol/L)	(Lin et al., 2013)
EIS	Z-scheme CdTe-Bi_2S_3 heterojunction play a role as effective visible-light-driven photoactive species	0.000005	0.00001–0.0995	sequence A	(Liu et al., 2017b)
EIS	AgI-nitrogen-doped graphene as recognition	0.0000169	0.00005–4.9759	sequence A	(Du et al., 2017)

convert photoirradiation to an electrical signal (Du et al., 2016b). In this way, various photocatalysts such as (Bismuth (III) sulphide (Bi_2S_3), Cadmium telluride (CdTe), and Bismuth oxybromide (BiOBr) have been utilized in PEC-based biosensors (Okoth et al., 2016).

For monitoring MC-LR in fish samples, a PEC aptasensor was fabricated with an LOD of 0.03 pM (Fig. 5). Here, BiOBr nanoflake/N-doped graphene (BiOBrNFs-NG) nanocomposites were immobilized on indium tin oxide (ITO) electrodes to provide a visible light-responsive material. The modified electrode was then subsequently biofunctionalized with an anti-MC-LR aptamer. The proposed sensing system was able to detect the target over a concentration range of 0.1 pM to 100 nM. RSD of resulting photocurrent was 3.46% (n = 5), reflecting the good reproducibility of the aptasensor. The overall recovery was 97.8–101.6% (Du et al., 2016b).

In another PEC based approach, an aptasensor capable of femtomolar detection of MC-LR was constructed using graphene functionalized titanium dioxide nanotubes (TiO_2 NTs). In the proposed system, alkyne-functionalized graphene was grafted onto azide-functionalized TiO_2 NTs, before the specific MC-LR aptamer (5-GGC GCC AAA CAG GAC CAC CAT GAC AAT TAC CCA TAC CAC CTC ATT ATG CCC CAT CTC CGC-3) was anchored onto the graphene surface. The aptasensor showed remarkable sensitivity (this is the most sensitive MC-LR aptasensor), with an LOD of 0.5 fM, as well as a direct dose-response relationship between target concentration and photocurrent over the range of 1.0–500 fM. The proposed system exhibited high and stable photocurrent and RSD was 0.3% after 6 cycles. The obtained RSD showed remarkable stability and repeatability of this sensing interface (Liu et al., 2016).

Engineered heterojunction photocatalysts demonstrate better photocatalytic performance, when compared with single component photocatalysts (Li et al., 2016a). This is due to the spatial separation of photogenerated electron–hole pairs provided by such heterostructures (Low et al., 2017b). Fabrication of direct Z-scheme photocatalyst is a promising strategy for elevation of photocatalytic efficiency. This technique optimizes reduction and oxidation potential of the photocatalytic component (Low et al., 2017a).

Exploiting these advantages, Liu and co-workers developed a PEC aptasensor with a LOD of 0.005 p.M. (Liu et al., 2017b). Herein, direct Z-scheme CdTe-Bi_2S_3 heterojunction played a role as an effective visible-light-driven photoactive species. In the proposed system, ITO electrodes were modified with CdTe-Bi_2S_3 heterojunctions. With the help of phosphor-amidate bonds, MC-LR aptamers were anchored onto the electrode surface. Over the range of 0.01–100 pM, the presence of the target led to dose-dependent decreases in PEC response. In addition, four independent electrodes (modified under the same condition) were incubated with 5 pM for calculation of RSD and reproducibility. An RSD of 7.3% was achieved and indicated suitable reproducibility of this aptasensor (Liu et al., 2017b).

More recently, Du and co-workers developed a PEC aptasensor with an LOD of 0.017 pM. The sensing platform produced by the MC-L|R aptamer and AgI-nitrogen-doped graphene, as recognition moiety and photocathode respectively, demonstrated linearity over a concentration range of 0.05 pM to 5 nM. When fish samples were spiked, recovery values ranged between 98.8% and 99.6%. The RSD of 4.2% (at the level of 5 nM)showed reproducibility of the aptasensor (Du et al., 2017).

In general, electrochemical aptasensors have several favorable features including reusability, requirement of low amounts of sample, and feasibility of quantitative analysis. These techniques still have important limitations. For instance, false positive results may be obtained due to the presence of matrix electrolytes. In addition, there is limited control on the working electrode, when higher currents are being induced (Nosrati et al., 2017). Table 2 presents the characteristics of electrochemical-based aptasensors.

4. Conclusion and future prospective

The potential hepatotoxicity of MC-LR means that monitoring of water quality and presence of MC-LR contamination in seafoods is highly necessary; the World Health Organization (WHO) has set an acceptable level of 1 $\mu g\,L^{-1}$ for MC-LR in drinking water. Development of sensitive and reliable analytical methods, that can ideally be deployed away from central laboratory facilities, is essential for the effective monitoring of MC-LR levels. Of the variety of different biosensing techniques explored to date, optical and electrochemical based systems have been repeatedly employed as aptasensors. Aptamers are used as recognition elements in aptasensors. In comparison with antibodies, aptamers exhibit higher affinity and selectivity towards their targets. Other desired features of aptamers are ease of production, high stability, and reproducibility.

Electrochemical systems possess numerous advantages including remarkable selectivity and simplicity as well as ease of operation. The ability to miniaturise and mass produce electrodes are further benefits of electrochemical systems.

As this review has revealed, construction of an ideal aptasensor depends on a number of different factors. Variations in the affinity and folding of aptamer sequences are important challenges in systems which rely on immobilization of aptamers on a solid surface such as an electrode. Although direct attachment of aptamers onto surfaces can lead to conformational changes, the use of spacer molecules can help overcome this problem.

The transduction system is another key factor that directly affects the sensitivity of aptasensor. For instance, through combining the advantages of graphene-functionalized titanium dioxide nanotubes and photoelectrochemical (PEC) technique, an ultrasensitive aptasensor with an LOD of 0.5 fM was fabricated.

Of the different aptasensors developed for the detection of MC-LR, those employing colorimetric readouts may be the simplest ones, with potential for assay results to be visible with the naked eye, however in comparison with other methods such sensors are often associated with relatively poor sensitivities.

Although remarkable advances have been made in aptasensor development over recent years, some major limitations remain before they are widely adopted. For example, sample specific issues such as total protein concentration, temperature and ionic strength may all influence the performance of aptamer biosensing. Noteworthy, aptamer-based biosensors are still in their infancy and some requirements must be met before these chemicals become commercially available and applicable.

With regards to widespread application of nanomaterials, combinations of biosensing technologies and microchip devices (microfluidic systems) are proposed as future platforms for simultaneous detection of MC congeners. Systems relied on lab-on-a-chip (LOC) and microfluidic technologies benefit from extraordinary throughput, portability and automation for several usages.

Acknowledgment

Financial support of this study was provided by Mashhad University of Medical Sciences.

Conflict of interest

None of the authors declare a conflict of interest.

References

Abnous, K., Danesh, N.M., Alibolandi, M., Ramezani, M., Taghdisi, S.M., Emrani, A.S., 2017a. Sens Actuators B Chem. 240, 100–106.
Abnous, K., Danesh, N.M., Ramezani, M., Taghdisi, S.M., 2017b. Microchim Acta. 184, 4451–4457.
Ansari, N., Wang, Z., Yazdian-Robati, R., Shahdordizadeh, M., Ghazvini, K., 2017. Anal. Biochem 533, 18–25.
Bilibana, M.P., Williams, A.R., Rassie, C., Sunday, C.E., Makelane, H., Wilson, L., Ntshongontshi, N., Jijana, A.N., Masikini, M., Baker, P.G., 2016. Sensors 16 (11), 1901.
Bini, A., Centi, S., Tombelli, S., Minunni, M., Mascini, M., 2008. Anal. Bioanal. Chem. 390 (4), 1077–1086.
Bostan, H.B., Danesh, N.M., Karimi, G., Ramezani, M., Shaegh, S.A.M., Youssefi, K., Charbgoo, F., Abnous, K., Taghdisi, S.M., 2017. Biosens. Bioelectron. 98, 168–179.
Bostan, H.B., Rezaee, R., Valokala, M.G., Tsarouhas, K., Golokhvast, K., Tsatsakis, A.M., Karimi, G., 2016. Life Sci. 165, 91–99.
Brosel-Oliu, S., Ferreira, R., Uria, N., Abramova, N., Gargallo, R., Muñoz-Pascual, F.-X., Bratov, A., 2017. Sens Actuators B Chem. 255, 2988–2995.
Chen, X.-M., Guo, G.-L., Sun, L., Yang, Q.-S., Wang, G.-Q., Zhang, D.-M., 2017. Fish. Physiol. Biochem 43, 1081–1093.
Cialla, D., Marz, A., Bohme, R., Theil, F., Weber, K., Schmitt, M., Popp, J., 2012. Anal. Bioanal. Chem. 403 (1), 27–54.
Corbel, S., Mougin, C., Bouaïcha, N., 2014. Chemosphere 96, 1–15.
Danesh, N.M., Bostan, H.B., Abnous, K., Ramezani, M., Youssefi, K., Taghdisi, S.M., Karimi, G., 2017. Trends Anal. Chem. 99, 117–128.
Du, X., Jiang, D., Dai, L., Zhou, L., Hao, N., Qian, J., Qiu, B., Wang, K., 2016a. Biosens. Bioelectron. 81, 242–248.
Du, X., Jiang, D., Dai, L., Zhou, L., Hao, N., Qian, J., Qiu, B., Wang, K., 2016b. Biosens. Bioelectron. 81, 242–248.
Du, X., Jiang, D., Hao, N., Qian, J., Dai, L., Zhou, L., Hu, J., Wang, K., 2016c. Anal. Chem. 88 (19), 9622–9629.
Du, X., Jiang, D., Li, H., Hao, N., You, T., Wang, K., 2017. Sens Actuators B Chem. 259, 316–324.
Eissa, S., Ng, A., Siaj, M., Zourob, M., 2014. Anal. Chem. 86 (15), 7551–7557.
Fisk, H., Westley, C., Turner, N.J., Goodacre, R., 2016. J. Raman Spectrosc. 47 (1), 59–66.
Gaget, V., Humpage, A.R., Huang, Q., Monis, P., Brookes, J.D., 2017. Water Res 124, 454–464.
Ghanbari, K., Roushani, M., Azadbakht, A., 2017. Anal. Biochem 534, 64–69.
Gu, K., Famulok, M., 2004. Zhonghua yu Fang. yi xue za zhi [Chin. J. Prev. Med.] 38 (6), 369–373.
Guo, L., Xu, Y., Ferhan, A.R., Chen, G., Kim, D.-H., 2013. J. Am. Chem. Soc. 135 (33), 12338–12345.
Hassanain, W.A., Izake, E.L., Schmidt, M.S., Ayoko, G.A., 2017. Biosens. Bioelectron. 91, 664–672.
Hayat, A., Sassolas, A., Marty, J.-L., Radi, A.-E., 2013. Talanta 103, 14–19.
He, Z., Wei, J., Gan, C., Liu, W., Liu, Y., 2017. RSC Adv. 7 (63), 39906–39913.
Herrero-Latorre, C., Álvarez-Méndez, J., Barciela-García, J., García-Martín, S., Peña-Crecente, R., 2015. Anal. Chim. Acta 853, 77–94.
High, B., Bruce, D., Richter, M.M., 2001. Anal. Chim. Acta 449 (1), 17–22.
Hosseini, M., Khabbaz, H., Dadmehr, M., Ganjali, M.R., Mohamadnejad, J., 2015. Acta Chim. Slov. 62 (3), 721–728.
Hu, L.-Y., Niu, C.-G., Wang, X.-y., Huang, D.-W., Zhang, L., Zeng, G.-M., 2017. Talanta 168, 196–202.
Jain, A., Homayoun, A., Bannister, C.W., Yum, K., 2015. Biotechnol. J. 10 (3), 447–459.
Jamali, A.A., Pourhassan-Moghaddam, M., Dolatabadi, J.E.N., Omidi, Y., 2014. Trends Anal. Chem. 55, 24–42.
Kaushik, R., Balasubramanian, R., 2013. Crit. Rev. Environ. Sci. Technol. 43 (13), 1349–1383.
La Porta, A., Sánchez-Iglesias, A., Altantzis, T., Bals, S., Grzelczak, M., Liz-Marzán, L.M., 2015. Nanoscale 7 (23), 10377–10381.
Li, H., Tu, W., Zhou, Y., Zou, Z., 2016a. Adv. Sci. 3, 11.
Li, Q., Lu, Z., Tan, X., Xiao, X., Wang, P., Wu, L., Shao, K., Yin, W., Han, H., 2017a. Biosens. Bioelectron. 97, 59–64.
Li, X., Cheng, R., Shi, H., Tang, B., Xiao, H., Zhao, G., 2016b. J. Hazard Mater. 304, 474–480.
Li, X., Zhang, X., Xie, W., Zhou, C., Li, Y., Zhang, X., 2017b. Toxicol. Vitr. 40, 115–123.
Lin, Z., Huang, H., Xu, Y., Gao, X., Qiu, B., Chen, X., Chen, G., 2013. Talanta 103, 371–374.
Ling, K., Jiang, H., Li, Y., Tao, X., Qiu, C., Li, F.-R., 2016. Biosens. Bioelectron. 86, 8–13.
Liu, J., Sun, Y., 2015. Toxicol. Lett. 236 (1), 1–7.
Liu, M., Ding, X., Yang, Q., Wang, Y., Zhao, G., Yang, N., 2017a. J. Hazard Mater. 331 (Supplement C), 309–320.
Liu, M., Yu, J., Ding, X., Zhao, G., 2016. Electroanalysis 28 (1), 161–168.
Liu, Q., Huan, J., Hao, N., Qian, J., Mao, H., Wang, K., 2017b. ACS Appl. Mater. Interfaces.
Liu, Y.-M., Zhou, M., Liu, Y.-Y., Huang, K.-J., Cao, J.-T., Zhang, J.-J., Shi, G.-F., Chen, Y.-H., 2014. Anal. Methods 6 (12), 4152–4157.
Lone, Y., Bhide, M., Koiri, R.K., 2016. J. Toxicol. 2, 289–296.
Lone, Y., Koiri, R.K., Bhide, M., 2015. Toxicol. Rep. 2, 289–296.
Low, J., Jiang, C., Cheng, B., Wageh, S., Al-Ghamdi, A.A., Yu, J., 2017a. Small Methods.
Low, J., Yu, J., Jaroniec, M., Wageh, S., Al-Ghamdi, A.A., 2017b. Adv. Mater. 29 (20).
Lundqvist, J., Pekar, H., Oskarsson, A., 2017. Toxicon 126, 47–50.
Lv, J., Zhao, S., Wu, S., Wang, Z., 2017. Biosens. Bioelectron. 90, 203–209.
Lyu, Y., Chen, G., Shangguan, D., Zhang, L., Wan, S., Wu, Y., Zhang, H., Duan, L., Liu, C., You, M., 2016. Theranostics 6 (9), 1440.
Ma, J., Feng, Y., Liu, Y., Li, X., 2016. Chemosphere 157, 241–249.
Ma, J., Li, Y., Duan, H., Sivakumar, R., Li, X., 2017. Chemosphere 192, 305–317.
McLellan, N.L., Manderville, R.A., 2017. Toxicol. Res (Camb.) 6 (4), 391–405.
Meirinho, S.G., Dias, L.G., Peres, A.M., Rodrigues, L.R., 2016. Biotechnol. Adv. 34 (5), 941–953.
Miller, A., Russell, C., 2017. Environ. Health Rev. 60 (3), 58–63.

Mosier-Boss, P.A., 2017. Biosensors 7 (4), 51.
Nakamura, C., Kobayashi, T., Miyake, M., Shirai, M., Miyakea, J., 2001. Mol. Cryst. Liq. Cryst. Sci. Tech. Mol. Cryst. Liq. Cryst. 371 (1), 369–374.
Ng, A., Chinnappan, R., Eissa, S., Liu, H., Tlili, C., Zourob, M., 2012. Environ. Sci. Technol. 46 (19), 10697–10703.
Nguyen, P.D., Son, S.J., Min, J., 2014. J. Nanosci. Nanotechnol. 14 (1), 157–174.
Nimjee, S.M., White, R.R., Becker, R.C., Sullenger, B.A., 2017. Annu Rev. Pharmacol. 57, 61–79.
Nosrati, R., Dehghani, S., Karimi, B., Yousefi, M., Taghdisi, S.M., Abnous, K., Alibolandi, M., Ramezani, M., 2018. Biosens. Bioelectron. 117, 1–14.
Nosrati, R., Golichenari, B., Nezami, A., Taghdisi, S.M., Karimi, B., Ramezani, M., Abnous, K., Shaegh, S.A.M., 2017. TrAC. Trends Anal. Chem. 97, 428–444.
Okoth, O.K., Yan, K., Liu, Y., Zhang, J., 2016. Biosens. Bioelectron. 86, 636–642.
Peuthert, A., Chakrabarti, S., Pflugmacher, S., 2007. Trends Anal. Chem. 22 (4), 436–442.
Pham, T.-L., Utsumi, M., 2018. J. Environ. Manag. 213, 520e529.
Qi, M., Dang, Y., Xu, Q., Yu, L., Liu, C., Yuan, Y., Wang, J., 2016. Chemosphere 157, 166–173.
Qileng, A., Cai, Y., Wei, J., Lei, H., Liu, W., Zhang, S., Liu, Y., 2018. Sens Actuators B Chem. 254 (Supplement C), 727–735.
Randviir, E.P., Banks, C.E., 2013. Anal. Methods 5 (5), 1098–1115.
Rezaitabar, S., Sari, A.E., Bahramifar, N., Ramezanpour, Z., 2017. Sci. Total Environ. 575, 1130–1138.
Rivas, L., Mayorga-Martinez, C.C., Quesada-González, D., Zamora-Gálvez, A., de la Escosura-Muñiz, A., Merkoçi, A., 2015. Anal. Chem. 87 (10), 5167–5172.
Rowland, C.E., Brown, C.W., Delehanty, J.B., Medintz, I.L., 2016. Mater. Today 19 (8), 464–477.
Sahoo, H., 2011. J. Photoch. Photobio. C 12 (1), 20–30.
Sekar, R.B., Periasamy, A., 2003. J. Cell Biol. 160 (5), 629–633.
Shahdordizadeh, M., Taghdisi, S.M., Ansari, N., Langroodi, F.A., Abnous, K., Ramezani, M., 2017. Sens Actuators B Chem. 241, 619–635.
Shuai, H.-L., Wu, X., Huang, K.-J., 2017. J. Mater. Chem. B 5, 5362–5372.
Smith, R., Wilson, J., Walker, J., Baskin, T., 1994. Planta 194 (4), 516–524.
Song, Y., Wei, W., Qu, X., 2011. Adv. Mater. 23 (37), 4215–4236.
Taghdisi, S.M., Danesh, N.M., Lavaee, P., Emrani, A.S., Ramezani, M., Abnous, K., 2015. RSC Adv. 5 (54), 43508–43514.
Taghdisi, S.M., Danesh, N.M., Ramezani, M., Ghows, N., Shaegh, S.A.M., Abnous, K., 2017. Talanta 166, 187–192.
Turner, A.D., Dhanji-Rapkova, M., O'Neill, A., Coates, L., Lewis, A., Lewis, K., 2018. Toxins 10 (1), 39.
Waldeisen, J.R., Wang, T., Ross, B.M., Lee, L.P., 2011. Acs Nano 5 (7), 5383–5389.
Wang, F., Liu, S., Lin, M., Chen, X., Lin, S., Du, X., Li, H., Ye, H., Qiu, B., Lin, Z., 2015. Biosens. Bioelectron. 68, 475–480.
Wang, Z., Yu, J., Gui, R., Jin, H., Xia, Y., 2016. Biosens. Bioelectron. 79, 136–149.
Wei, J., Qileng, A., Yan, Y., Lei, H., Zhang, S., Liu, W., Liu, Y., 2017. Anal. Chim. Acta 994 (Supplement C), 82–91.
Woods, J.M., Jung, Y., Xie, Y., Liu, W., Liu, Y., Wang, H., Cha, J.J., 2016. ACS nano 10 (2), 2004–2009.
Wu, S., Duan, N., Zhang, H., Wang, Z., 2015. Anal. Bioanal. Chem. 407 (5), 1303–1312.
Yi, S., Sun, L., Lenaghan, S.C., Wang, Y., Chong, X., Zhang, Z., Zhang, M., 2013. RSC Adv. 3 (26), 10139–10144.
Zanato, N., Talamini, L., Silva, T.R., Vieira, I.C., 2017. Talanta 175, 38–45.
Zegura, B., 2016. Mini Rev. Med Chem. 16 (13), 1042–1062.
Žegura, B., Štraser, A., Filipič, M., 2011. Mutat. Res Rev. Mutat. Res 727 (1), 16–41.
Zhang, L., Meng, X., Xiang, Z., Li, D., Han, X., 2017a. Toxicol. Sci.
Zhang, Y., Chen, M., Li, H., Yan, F., Pang, P., Wang, H., Wu, Z., Yang, W., 2017b. Sens Actuators B Chem. 244, 606–615.
Zhao, Y., Yang, X., Li, H., Luo, Y., Yu, R., Zhang, L., Yang, Y., Song, Q., 2015. Chem. Comm. 51 (95), 16908–16911.
Zhou, H., Liu, J., Xu, J.-J., Chen, H.-Y., 2011. Chem. Comm. 47 (29), 8358–8360.